ARTICLE

Photo-induced Intra-complex Reactions in Ca^+-Pyridine

Dong-sheng Wang[a,b*], Ke-li Han[b], Shi-he Yang[a]

a. Department of Chemistry, The Hong Kong University of Science and Technology, Hong Kong, China; b. State Key Laboratory of Molecular Reaction Dynamics, Dalian Institute of Chemical Physics, Chinese Academy of Science, Dalian 116023, China

(Dated: Received on February 4, 2005; Accepted on May 22, 2005)

Photodissociation spectra of Ca^+-pyridine complex was obtained by reflectron time of flight spectrum (RTOF). Two channels were found from difference photodissociation spectra, one was non-reactive Ca^+ cation separation channel, the other one was active channel for product Ca^+NH_2. Product Ca^+ was dominant in the whole region studied and the only product in 530-590 nm region, reactive product Ca^+NH_2 shared a little present in whole products. Action spectrum as a function of photolysis laser wavelength shows appearance peaks relevant to transitions of complex. Branching ratio supports the information of photodissociation too.

Key words: Complex, Photodissociation, Action spectrum

I. INTRODUCTION

Photodissociation of bimolecular complexes of simple metal ions with molecules plays an important role in a wide range of biological, chemical, and physical processes [1-13]. It often gives valuable information about the complex structure and the intermolecular interactions [2-8]. It is also a powerful tool to detect the dynamics of half-collision bimolecular reactions [9-13]. Singly charged alkaline earth metal cations are involved in many experiments and theoretical studies, because they have only one valence electron just like the alkali metal atoms. The intense atomic resonance is easily accessed by visible and ultraviolet laser sources. With the rapid development of the experiment techniques, many studies have been conducted on the photodissociation of the alkaline earth cation-molecule complexes [3-13]. Our group has reported a number of intra-complex reactions, including C−F, C−O, C−N, and N−H bond activations and charge transfer (CT), by means of photodissociation of the Mg^+-molecule complexes.

Pyridine is one of the most abundant and best known of aromatic heterocyclics. Compounds containing pyridine ring are widely distributed in nature, principally as enzymes and alkaloids. Pyridine enzymes have been found in tissues of all plants and animals examined thus far, and are derived from either nicotinic acid or Vitamin B_6 [14]. Pyridine is also a building block of many pharmaceutical with a wide range of functionalities that include anti-tubercular compounds, antiviral and antitumor agents, central nervous system stimulants, diagnostic agents, analgesics, anti-inflammatory agents, and antihistamines [15,16]. As a whole, Mg^+-pyridine is an ideal model for studying non-covalent interactions of metal ions with a large range of nitrogen containing heterocyclics of biological importance.

Much work has been done on the reactions of M^+-pyridine. Rodgers *et al.* [17,18] used threshold collision induced dissociation and density functional theory to study periodic trends in the binding of M^+-pyridine (M=Mg, Al, Sc, Ti, V, Cr, Mn, Fe, Co, Ni and Zn; Li, Na and K). Our group has reported photon dissociation of M^+-pyridine recently [19]. In addition to a non-reactive channel, a photodissociation CT reaction channel was identified and thought to result from curve crossing between $3p_z$ and CT states. For comparison, the photo-induced reaction of Ca^+-pyridine has now been studied, which will be reported here. CT reaction was not found in Ca^+-pyridine photodissociation. However, an interesting reactive channel was identified in this process. The study of this difference may give some useful information on the nature of the photoreactions.

II. EXPERIMENT AND RESULTS

The experimental apparatus has been depicted previously [7,10] and thus only the parts relevant to the present experiments are given here. A rotating Calcium-oxide rod attached to a sample holder was mounted 15 mm downstream from the exit of a pulsed valve (General Valve). Driven by a step motor, the sample disk rotated on each laser pulse to expose the fresh surface during the laser-ablation experiments. The pulse valve was used to generate a beam of pyridine by supersonic expansion of a gas mixture of pyridine vapor seeded in helium carrier gas (with a backing pressure of ∼40 psi) through a 0.5 mm diameter orifice. The second

*Author to whom correspondence should be addressed. E-mail: dswang_cn@yahoo.com.cn

harmonic (532 nm) of a Nd:YAG laser (∼40 mJ/pulse) was weakly focused on a ∼1 mm diameter spot of the Calcium-oxide disk for the generation of metal cations. The laser-vaporized species traversed the supersonic jet stream 20 mm from the ablation sample target, forming a series of solvated metal cation-pyridine cluster complexes. The clusters thus formed traveled 14 cm downstream to the extraction region of the reflection time-of-flight spectrometer (RTOFMS).

The cation-molecule complexes were accelerated vertically by a high-voltage pulse (∼1000 V in amplitude and 25 μs in width) in a two-stage extractor. After extraction, the cation-molecule complexes were steered by a pair of horizontal plates and a pair of vertical deflection plates. All the cluster cations were reflected by the reflectron (VR1=+650 V, VR2=+1050 V) and finally detected by a dual-plate microchannel detector (MCP). For photodissociation experiments, a two-plate mass gate equipped with a high-voltage pulser (normally at +500 V) was used to select desired cluster cations. The mass-selected cluster cations, once arriving at the turn-around region of the reflectron, were irradiated with a collimated beam of a dye laser for photolysis. The parent and nascent daughter cations were re-accelerated by the reflectron electric field and detected by the MCP detector. The dye laser for photodissociation was pumped by a XeCl excimer laser (Lambda Physik LPX 210i/LPD3002). The spectral region of 412-690 nm was covered by the fundamental outputs of the dye laser using stilbene 420, Coumarin 460, Coumarin 503, Coumarin 540A, Kiten Red, DCM. The photolysis laser fluence was kept low (<1 mJ/cm^2) to avoid multiphoton processes and saturation phenomena.

The photodissociation difference mass spectra of the complex at 466 nm (a) and 560 nm (b), as shown in Fig.1, were obtained by subtracting collected data taken with and without the photodissociation laser on. Thus, the negatively oriented peaks indicate the disappearance of the parent complex, and the positively oriented peaks correspond to the appearance of daughter ions. Judging from the photodissociation mass spectra in Fig.1, Ca^+ persists in the entire spectral region we studied (412-690 nm), and is the dominant production throughout the spectral region and the only channel observed between 530-590 nm. According to the spectra, there are two channel products: a non-reactive channel product Ca^+ and a reactive channel product Ca^+NH_2 as shown in Fig.1.

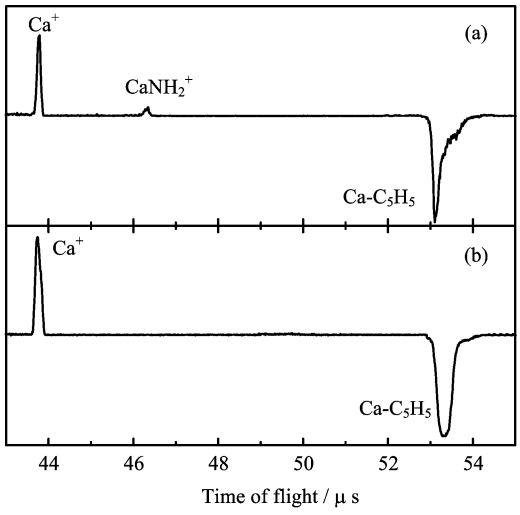

FIG. 1 Photodissociation difference mass spectra of Ca^+-pyridine at (a) 466 nm and (b) 560 nm.

Figure 2 shows the action spectrum of Ca^+-pyridine in the wavelength range of 412-690 nm, in which the total ion yield of the photofragments was monitored as a function of the photolysis laser wavelength, and normalized by the parent ion intensities and laser fluence. The action spectrum consists of three continuous bands peaked about at 477 nm (FWHM ∼20 nm), 592 nm (FWHM ∼20 nm), and 650 nm (FWHM ∼18 nm). And the peak of ∼592 nm has a pre-tail. The observed peaks in the action spectrum apparently originate from the splitting of the $4^2P \leftarrow 4^2S$ atomic transition of Ca^+. The splitting is primarily due to the alignments of the three 3p orbitals in the excited states of Ca^+ with respect to the pyridine ligand.

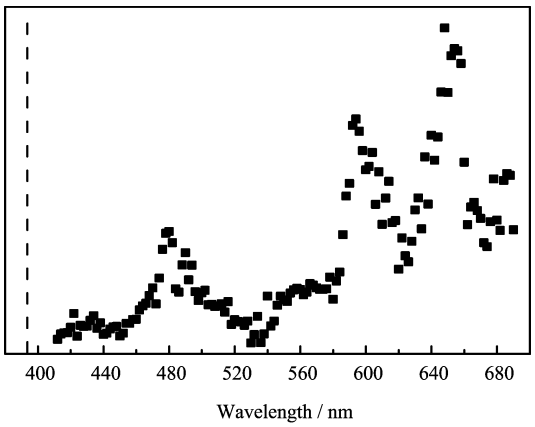

FIG. 2 Action spectrum of Ca^+-pyridine. The vertical axis represents the total photofragment ion yield. The dotted line indicates the atomic transition of $Ca^+(^2P \leftarrow {}^2S)$.

Figure 3 gives the fragment branching fractions as a function of laser wavelength. The Ca^+ is the only observed product when the laser wavelength is within the range of 530-590 nm. And the reactive channel product has two peaks, one is at about 440 nm, and the other at about 605 nm. This is different from the Mg^+-pyridine photoreaction. Aside form a charge transfer (CT) except the Mg^+ separation channel, the photodissociation of Mg^+-pyridine has no reactive channel. This may be due to the higher reactivity of Ca^+.

In order to unravel the photodissociation mechanism, GAUSSIAN 98 package was used to do the *ab initio* calculations. The ground-state geometry of Ca^+-pyridine complex, pyridine, and other reaction products were fully optimized at the B3LYP/6-311++G** level. Figure 4 shows the calculated ground-state geometry of Ca^+-pyridine complex. Ca^+ bonded to the nitrogen

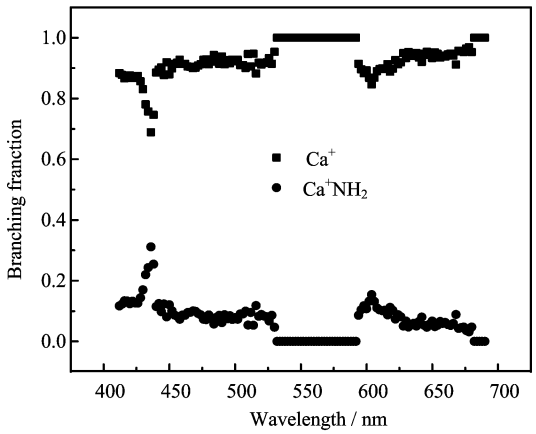

FIG. 3 Photofragment branching fractions from Ca^+-pyridine as a function of the laser wavelength.

atom at the side of the pyridine ring. This is the same geometry as the Mg^+-pyridine complex. The calculated Ca^+-pyridine bond length is 2.403 Å, longer than the Mg^+-N bond length (2.133 Å). On the basis of the computational result for the ground state, vertical excitation energies to the low-lying excited states of Ca^+-pyridine complex were calculated using the CIS method. In Fig.2, the three bands of the complex are peaked

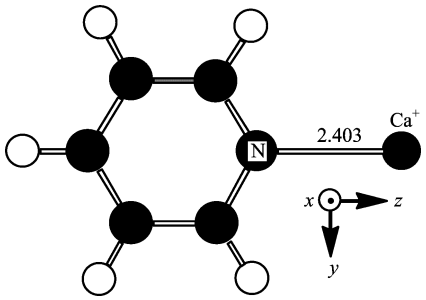

FIG. 4 Optimized ground-state structure of the Ca^+-pyridine complex at the B3LYP/6-311++G** level.

about at 477, 592, 650 nm. The calculated three transitions (4P type) are 512.8, 540.5 and 575.3 nm, respectively, and correspond to $4p_z, 4p_y, 4p_x$ states. The calculated values have about 10% deviation from the experimental data, but the calculation at least can give us a guide to estimate the general trends of the properties in question. Thus, we can assign the bands about at 477 nm as $4p_z$ transition, 592 nm as $4p_y$ transition, and 650 nm as $4p_x$ transition. And before these three bands, there is a little band at the shorter wavelength peaked about at 430 nm. Calculations show that in this region, weak transitions of the complex mainly focus on the pyridine ring. The electronic excitations are more likely to open the pyridine ring: the recoil of the N atom is accompanied by the capture of the two neighboring H atoms, leading to the formation of Ca^+NH_2. Thus the fragment branching fractions in this region shows a peak of Ca^+NH_2. However, since the pyridine ring is very stable, it is difficult to open the ring and this explains the low yield of the reactive product and the dominant non-reactive channel. We suggest that the non-reactive channel is the result of pre-dissociation, which involves internal conversion from the original excited state to the ground state. This type of *E-V* quenching mechanism has been discussed extensively in the scientific literature.

III. ACKNOWLEDGMENT

We are grateful to the Research Grants Council of Hong Kong and HKUST for financial support of the research.

[1] C. Desfrancois, S. Carles, and J. P. Schermann, Chem. Rev. **100**, 3943 (2000).
[2] M. A. Duncan, Annu. Rev. Phys. Chem. **48**, 69 (1997).
[3] P. D. Kleiber and J. Chen, Int. Rev. Phys. Chem. **17**, 1 (1998).
[4] S. S. Wesolowski, A. K. Rollin, H. F. Schaefer III and M. A. Duncan, J. Chem. Phys. **113**, 701 (2000).
[5] W. Y. Lu and P. D. Kleiber, J. Chem. Phys. **114**, 10288 (2001).
[6] L. N. Ding, P. D. Kleiber, Y. C. Cheng, M. A. Young, S.V. Oneil and W. C. Stwalley, J. Chem. Phys. **102**, 5235 (1995).
[7] W. Y. Guo, H. C. Liu and S. H. Yang, J. Chem. Phys. **116**, 9690 (2002).
[8] C. W. Bauschlicher, Jr., M. Sodupe and H. Partridge, J. Chem. Phys. **96**, 4453 (1992).
[9] J. Chen, T. H. Wong, Y. C. Cheng, K. Montgomery and P. D. Kleiber, J. Chem. Phys. **108**, 2285 (1998).
[10] H. C. Liu, C. S. Wang, W. Y. Guo, Y. D. Wu and S. H. Yang, J. Am. Chem. Soc. **124**, 3794 (2002).
[11] W. Y. Guo, H. C. Liu and S. H. Yang, J. Chem. Phys. **116**, 2896 (2002).
[12] H. M. Yin, J. L. Sun, Y. M. Li, G. Z. He and K. L. Han, Chem. Phys. Lett. **356**, 601 (2002).
[13] C. S. Yeh, J. S. Pilgrim, K. F. Willey, D. L. Robbins and M. A. Duncan, Int. Rev. Phys. Chem. **13**, 231 (1994).
[14] F. Brody, P. R. Ruby, in: E. Klingsberg (Ed.), *Heterocyclic Compounds, Pyridine and Derivatives*, Part 1, Interscience Publishers, New York 99, (1960).
[15] R. T. Coutts, A. F. Casy, in: R. A. Abramovitch (Ed.), Pyridine and Its Derivatives, Suppl., Part 4, John & Sons, New York, 445, (1975).
[16] T. L. Gilchrist, *Heterocyclic Chemistry*, 3rd ed., Longman Singapore Publisher Inc., Singapore 125, (1997).
[17] M. T. Rodgers, J. R. Stanley and R. Amunugama, J. Am. Chem. Soc. **122**, 10969 (2000).
[18] R. Amunugama and M. T. Rodgers, Int. J. Mass. Spectrom. **195**, 439 (2000).
[19] W. Y. Guo, H. C. Liu and S. H. Yang, Int. J. Mass. Spectrom. **226**, 291 (2003).